scientific reports

Check for updates

OPEN

Development of hybrid green nanocomposite polymeric beads doped with nano sulfated zirconia for effective removal of Cefotaxime antibiotic from aqueous solution

Marwa H. Gouda[1], Noha A. Elessawy[2]✉ & Arafat Toghan[3,4]

Adsorption efficiency of *Cefotaxime* by novel nanocomposites beads composed of iota carrageenan (IC), sulfonated poly vinyl alcohol (SPVA) and nano sulfated zirconia ($SZrO_2$) was evaluated in this study. $SZrO_2$ was synthesized from solvent-free and easy calcination technique then embedded with 1–2.5 wt.% into the polymeric matrix. A batch adsorption experiment was carried out to investigate the effects of dosage, pH, beginning concentration, and time on *Cefotaxime* antibiotic adsorption. The ideal conditions to achieve complete removal are 88.97 mg L^{-1} initial cefotaxime concentration at time 3.58 h with 11.68 mg of beads composite with 2.5 wt.% of $SZrO_2$. The pseudo second order kinetics model better illustrated the adsorption of cefotaxime on nanocomposite beads, and the maximum adsorption capacity are 659 mg g^{-1} for the composite with 2.5 wt.% of $SZrO_2$. The mechanism of adsorption process depend mainly on the interactions between the different functional groups of SPVA, IC and $SZrO_2$. The nanocomposites beads also exhibit excellent reproducibility after ten adsorption cycles. This type of nanocomposites beads can be easily separated from water without leaving any residue, verifying this novel nanocomposite beads has strong potential in water treatment for the antibiotic contaminant removal.

Water treatment processes confront significant challenges in terms of optimizing technology to avoid human health concerns and to ensure environmental sustainability, as population grows, water sources become scarcer and water quality deteriorates due to land use and climate change[1]. These water-related issues are better understood and handled as a result of enhanced detection and awareness of the toxicological, environmental, and biological effects of an ever-growing list of substances dubbed Emerging Pollutants (EPs). EPs are a group of man-made chemicals, such as pharmaceuticals, pesticides, flame retardants, detergents, and cosmetics, that are essential to contemporary living and whose manufacture and use have risen dramatically in the previous decades[1–3]. The uncontrolled and continuous release of these new compounds into the environment may have an impact on aquatic biota, human health[4,5] and also the performance and costs of drinking water treatment technologies[6,7].

Antibiotics are classified as a type of persistent pollutant that lead to fast spread of different types of resistant bacteria. *Cefotaxime* is important type of cephalosporin antibiotics for the treatment of gram negative and positive bacterial infections with a lengthy half-life owing to its aromatic-ring structure. It is usually detected in wastewater and drinking water and is very difficult to totally remove[8]. Nowadays, there are different techniques have been applied to eliminate antibiotics from aquatic system, such as oxidation[9], adsorption and degradation[10,11]. Between these techniques, adsorption is cheap, simple, promising method for antibiotics, organic and inorganic contaminants removal from water[12–15]. The polymeric beads as adsorbent have been more favorable than the

[1]Polymer Materials Research Department, Advanced Technology and New Materials Research Institute (ATNMRI), City of Scientific Research and Technological Applications City (SRTA-City), Alexandria 21934, Egypt. [2]Computer Based Engineering Applications Department, Informatics Research Institute IRI, City of Scientific Research & Technological Applications (SRTA-City), Alexandria 21934, Egypt. [3]Chemistry Department, Faculty of Science, South Valley University, Qena 83523, Egypt. [4]Chemistry Department, College of Science, Imam Mohammad Ibn Saud Islamic University (IMSIU), Riyadh 11623, Saudi Arabia. ✉email: nony_essawy@yahoo.com

nanoparticles, film or fiber forms because of its easy fabrication, excellent dispersion, controllable size dimension and quick recovery process.

Carrageenan is a sulfated polysaccharide made up of anhydrogalactose and galactose units found in red seaweed extracts[16]. Iota carrageenan is the most often utilized, which comprise two sulfated groups per disaccharide unit. Because of its chemical functionality and natural abundance, it is widely used for water treatment, namely in the removal of pharmaceutical contaminants and pesticides[17].

Poly vinyl alcohol (PVA) is an eco-friendly, biodegradable and cost-effective polymer with outstanding chemical stability and hydrophilicity properties; therefore, it is widely used to eliminate various pollutant from water. This type of polymer contains abundant hydroxyl groups and can be easily coagulated and cross-linked, however, by mixing PVA with IC lead to create porous network rich with hydroxyl and sulfate groups, which can be effective for the adsorption capacity enhancement[18].

The presence of metal oxide nanostructures in the surface and structure of polymeric matrix leads to the production of nanocomposite polymeric-based matrix, which has been proposed as one of the most potent tools for preventing membrane fouling in various water treatment processes[19–23]. Among metal oxide nanoparticles, ZrO_2 has received a lot of interest in recent years due to its unique properties such as good chemical and mechanical stability with high hydrophilic properties, in addition to their availability, low cost and simple synthesis method[21]. However, sulfated zirconia as the adsorbent consider as a cation exchanger that promotes more elimination of the cationic counterpart such as wide sector of antibiotics which contain amine groups.

This work aimed to synthesis eco-friendly and effective green adsorbent nanocomposite beads prepared by using water as a solvent to process biodegradable and low-cost polymers to remove *Cefotaxime* antibiotic contaminant from water. PVA was chosen as the key polymer in the beads due to its good interaction with IC polymer to form compatible composite rich with functional groups, in addition to supporting $SZrO_2$ nanoparticles. To our knowledge, this is the first time to $SZrO_2$ nanoparticles have been incorporated into PVA/IC blending polymers matrix in different concentrations to create nanocomposite beads named as SPVA/IC/$SZrO_2$ and use it as adsorbent for antibiotics in water treatment.

Experimental

Iota carrageenan (type V), PVA (99% hydrolysis and medium MW), *Cefotaxime* sodium salt and 4-sulphophthalic acid (SPA) (99.9 wt.% in H_2O) were purchased from (Sigma-Aldrich, USA) and Glutaraldehyde (GA) (50 wt.% in H_2O) was purchased from Alfa Aesar.

Synthesize. *Synthesize of nano-sulfated zirconia ($SZrO_2$).* Nano $SZrO_2$ was prepared using a simple calcination method in the absence of any solvent between zirconium oxychloride octahydrate $ZrOCl_2.8H_2O$ and ammonium sulfate $(NH_4)_2SO_4$ with 1:5 molar ratio were mixed and ground in a mortar then placement for 12 h at room temperature, after that calcined for 5 h at 600 °C. Finally, the powder was ground in ball mill at 1500 rpm for 30 min to obtain nano size.

Preparation of SPVA/IC/$SZrO_2$ beads. First, PVA and IC were dissolved separately in 100 mL deionized H_2O at 90 °C for 2 h then blending with percentage PVA: IC (95:5) wt.%. After that, crosslinking the polymers blend by certain amount of GA as covalent crosslinker and SPA as ionic crosslinker and sulfonating agent for PVA, to convert to sulfonated polyvinyl alcohol (SPVA)[22]. Then the prepared nanocomposite was incorporated with different concentrations of $SZrO_2$ (1wt.% and 2.5wt.%) in polymeric blend. The two solution samples were named SPVA/IC/$SZrO_2$-1, SPVA/IC/$SZrO_2$-2.5. The composite solution was put in syringe, dropped in saturated solution of boric acid to form beads, and left for overnight then washing.

As illustrated in Fig. S1 in supplementary information which shows the possible structure of SPVA/ IC/ $SZrO_2$ beads, esterification reactions between carboxylic groups of SPA and hydroxyl groups of two polymers were used to ionically crosslink IC and PVA. Furthermore, acetal interactions between GA's aldehyde groups and the hydroxyl groups of the two polymers covalently crosslinked the two polymers. While $SZrO_2$ was bonded to polymeric matrix by hydrogen bond interactions between its oxygenated groups and the -OH groups of two polymers.

Characterization. The characteristic groups of $SZrO_2$ powder and the nanocomposite beads were monitored by Fourier transform infrared spectrophotometer (Schimadzu FTIR-8400 S-Japan), while the structures were evaluated by X-ray diffractometer (Schimadzu7000-Japan). Thermal changes of SPVA/IC/$SZrO_2$ beads were traced by using thermo-gravimetric analyzer (Shimadzu TGA-50, Japan) the range of the temperature was 25–800 °C, under nitrogen atmosphere and the heating rate at 10 °C min^{-1}. Morphological structure of the SPVA/IC/$SZrO_2$-2.5 beads was shown by scanning electron microscope (SEM) combined with energy-dispersive analysis X-ray (EDX) (Joel Jsm 6360LA-Japan). Visualization of the nano $SZrO_2$ was done by using transmission electron microscopy (TEM, JEM 2100 electron microscope).

To investigate the beads stability, pieces with diameter of 1 mm were immersed in 100 mL of deionized water at 35℃ for 24 h. The swelling coefficient S was calculated as follows:

$$S(\%) = \frac{W_w - W_d}{W_d} \times 100 \quad (1)$$

where W_w and W_d were the masses of the swollen and dry PVA/IC/$SZrO_2$ nanocomposite bead, respectively.

To determine the point of zero charge (pHpzc) of PVA/IC/$SZrO_2$ nanocomposite bead, 5 mg of beads were added up to 10 mL of solutions containing the pH values ranging from 3 to 9. The suspensions were then shaken gently for 24 h, then final pH values of every solution were recorded and the pH_{PZC} values was calculated.

Model	Linear form	Eq. no	Plot	Parameters and constants
Pseudo-first-order kinetic	$\ln (q_e - q_t) = \ln q_e - k_1 t$	(5)	$\ln(q_e - q_t)$ vs. t	k_1 is the pseudo-first-order adsorption rate constant; q_e is the amount of antibiotic adsorbed at saturation per gram of adsorbent (mg g^{-1}), q_t is the amount of antibiotic adsorbed at time t per gram of adsorbent (mg g^{-1})
Pseudo second-order kinetic	$\frac{t}{q_t} = \left[\frac{1}{k_2 qe^2}\right] + \frac{1}{q_e} t$	(6)	t/q_t vs. t	k_2 is adsorption rate constant of the pseudo-second-order
Intraparticle diffusion kinetic	$q_t = k_i t^{1/2} + C$	(7)	q_t vs. $t^{1/2}$	k_i (mg g^{-1} $min^{-1/2}$) is the intraparticle diffusion rate constant, which is the slope of the straight line of q_t versus $t^{1/2}$; C is the value of intercept, which is a constant reflecting the significance of the boundary layer or mass transfer effect
Langmuir isotherm	$\frac{q_e}{C_e} = \frac{1}{K_L q_m} + \frac{C_e}{q_m}$	(8)	(C_e/q_e) vs. C_e	q_e is the solid-phase concentration in equilibrium with the liquid-phase; concentration C_e is expressed in mole L^{-1}; q_m is the maximum monolayer adsorption capacity (mg g^{-1}); and K_L is an equilibrium constant (L mol^{-1})
Freundlich isotherm	$\ln q_e = \ln K_f + \frac{1}{n} \ln C_e$	(9)	ln q_e vs. ln C_e	plotting ln q_e versus ln C_e gives a straight line with slope of 1/n, where n is a constant related to adsorption intensity and its magnitude shows an indication of the favorability of adsorption; the intercept is ln K_f where K_f is constant (function of energy of adsorption and temperature)

Table 1. Kinetics and isotherms models of adsorption process.

Batch adsorption tests. Adsorption tests were carried out by using a batch equilibration technique. One gram per liter stock solutions of *Cefotaxime* antibiotic were diluted to different degrees by adding deionized water. However, 50 mL of *Cefotaxime* antibiotic solutions with different concentrations (25, 50,100 and150 mg L^{-1}) at 25 °C were added with a specific amount of prepared nanocomposite beads, with the help of a thermostated shaker running at 150 rpm. After reaching equilibrium, the adsorbent beads were separated and the remaining antibiotic concentration in the aqueous phase was measured using a UV spectrophotometer at 235 nm.

The amounts of adsorbed antibiotic were calculated according to the following formulas:

$$q_t = \frac{C_0 - C_t}{m} V \tag{2}$$

$$q_e = \frac{C_o - C_e}{m} V \tag{3}$$

where qt and qe (mg g^{-1}) were the amounts of antibiotic adsorbed per unit weight of adsorbent at time t and equilibrium; C_0, C_t and C_e mg L^{-1} were the antibiotic concentrations at initial time, time t and the equilibrium time, respectively; V (L) was the volume of antibiotic solution; and m (g) was the amount of adsorbent. The removal efficiency R was determined as follows:

$$R(\%) = \frac{C_0 - C_t}{C_0} \times 100 \tag{4}$$

To optimize the *Cefotaxime* antibiotic removal conditions, we tried to establish a relationship between factors and responses, according to a response surface methodology (RSM) model. The selected matrix for the response surface methodology followed the Box-Behnken design[24], with 17 trials. To evaluate the adsorption process performance, three factors were used: A (time, min); B (initial antibiotic concentration, mg L^{-1}); and C (beads adsorbent dose, mg), at three levels illustrated in Table S1 in supplementary information. Design-Expert, 13.0.9.0 programme from STAT-EASE, INC was used for experimental design, model construction and data analysis. After proper optimization of the adsorption, the kinetic and isotherm parameters of the process were characterized.

Static kinetics and isotherms models of adsorption. The rate and mechanism of the adsorption process could be elucidated based on kinetic studies with different initial concentrations of *Cefotaxime* antibiotic varied from 25 to 150 mg L^{-1}. The pH was fixed at 5 and dose of adsorbent was 2 mg mL^{-1}, while the adsorption time was varied from 0 to 24 h. In order to elucidate the adsorption kinetics, the pseudo-first-order, pseudo second-order and intraparticle diffusion models were applied, as illustrated in Table 1. Additionally, to describe how the adsorbate interacts with adsorbents and give a thorough understanding of the nature of interaction, the adsorption isotherm models were tested to validate the antibiotic uptake behavior of PVA/IC/$SZrO_2$ composite bead using Langmuir and Freundlich isotherms.

Reusability test. To investigate the reusability of PVA/IC/$SZrO_2$ composite bead, 10 mg of beads was mixed with 50 mL of 20 mg L^{-1} antibiotic. The mixture was shaken for 15 min. after adsorption, the beads was separated. Then 0.01 M NaOH was added and the solution was shaken again for 15 min. Finally, the beads was repeatedly washed by 70% (v/v) ethanol aqueous solution, until antibiotic was no longer detected in the solution. The cyclic adsorption–desorption processes were conducted up to 10th cycle successfully to study the reusability of the nanocomposite.

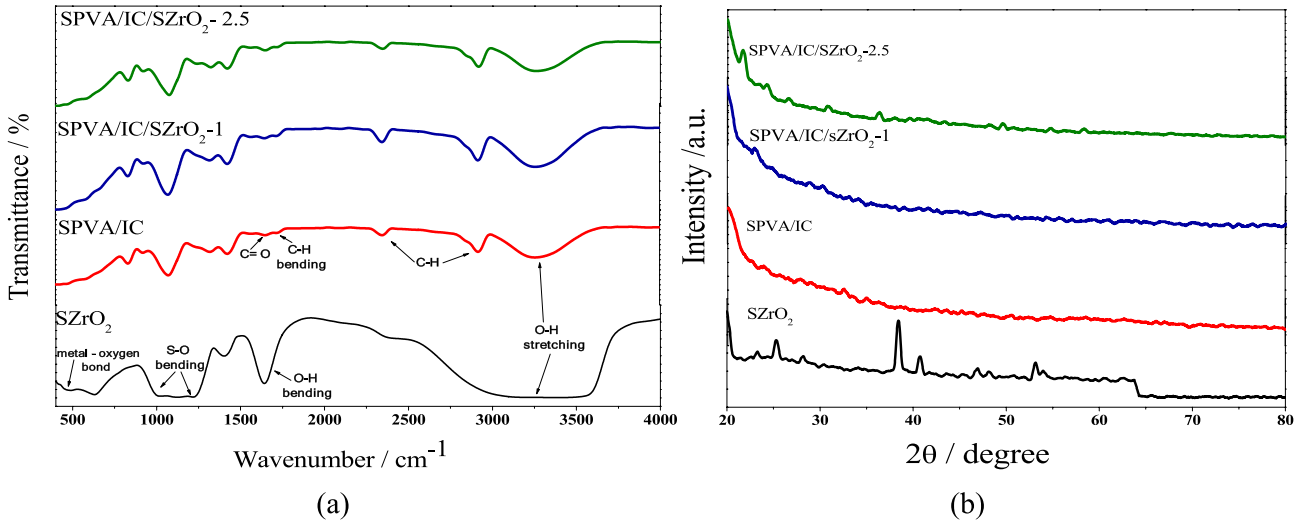

Figure 1. (**a**) FTIR spectra of $SZrO_2$ and SPVA/IC/SO_4ZrO_2 composite beads, (**b**) XRD patterns of $SZrO_2$ and SPVA/IC/ $SZrO_2$ composite beads.

Results and discussion

Morphological, physical and thermal characteristics of $SZrO_2$ and nanocomposite beads. Figure 1a illustrate FTIR spectra of $SZrO_2$ and PVA/IC/$SZrO_2$ composite beads. $SZrO_2$ spectrum shows a board peak at 3250 cm^{-1} and sharp peak at 1630 cm^{-1}, that may be referred to the adsorbed moisture and hydrogen bonds formed, however, the peak around 500 cm^{-1} return to Zr–O bond, while, peaks at 1217, 1128 and 1016 cm^{-1} are characteristic for S–O. On the other hand, the FTIR spectra for PVA/IC/ $SZrO_2$ nanocomposite beads, the bands around 3250 cm^{-1} are attributable to the O–H bonds from water molecules that become more adsorbed as the concentration of sulfated zirconia increases due to its hydrophilic properties, and the bands at 1600 cm^{-1} are indicative of –OH groups of PVA and IC. The sulphate groups of iota carrageenan have a distinctive peak at 830 cm^{-1}. The C–H bonds in the polymers structure can be attributed to bands at 2840 and 2300 cm^{-1}[25], while the weak bands at 1700 and 1750 cm^{-1} correspond to C=O bonds and C–H bending, respectively in the aromatic structure of sulfophithalic acid (SPA), which demonstrate that the crosslinking process has been completed. Sulfate groups of $SZrO_2$ are responsible for the bands at 950 and 1100 cm^{-1}.

In Fig. 1b it can be observed the amorphous structure for the prepared composite beads increased with increasing $SZrO_2$ concentration, while the sulfated zirconia powder curve shows characteristic peaks intensity of $SZrO_2$ at a 2θ angle 54, 28, 38[26,27].

Figure 2a shows a semi-spherical shape for SPVA/IC/SO_4ZrO_2 composite beads and porous future for inside surface Fig. 2b. While the TEM image of sulfated zirconia in Fig. 2c demonstrated that, the material developed in nanoscale particles. EDX spectra as shown in Fig. 2d confirmed the presence of sulphur groups on the surface of $SZrO_2$, proving the synthesize of sulfated zirconia.

As shown in Fig. 3, the TGA curves of beads without and with $SZrO_2$shows about 8% loss in weight at ~ 150 °C and that returns to the moisture evaporation[21]. The second loss stage of composite beads occurred in the range of 150—270 ℃ and is related to the degradation of functional groups, while the third loss stage is characterized by a remarkable decomposition from 270 to 360 ℃ and is related to the decomposition of polymeric chains, which began at 230 ℃ for the undoped beads and at 270 ℃ with a lower weight percentage for the doped beads. This behaviour demonstrates that the addition of $SZrO_2$ improves the composite's temperature stability by boosting covalent, ionic, and hydrogen bonding in the nanocomposite.

As shown in Fig. 3b, response of swelling behavior of SPVA/IC, SPVA/IC/$SZrO_2$-1 and SPVA/IC/$SZrO_2$-2.5 in water with respect to time was studied at room temperature. After a set amount of time had passed, the degree of swelling was assessed, and the immersion experiment lasted 24 h. SPVA/IC beads showed maximum degree of among other beads with $SZrO_2$ and that can be explained by adding $SZrO_2$ to the polymeric mixture of SPVA and IC may result in an increase in the amount of hydrogen bonds formed between polymer chains and $SZrO_2$, resulting in increased chemical stability in polymer chains.

Adsorption process evaluation. *Effect of solution pH and adsorption surface chemistry.* It is crucial to investigate the beads' main surface charge at a certain pH. The calculation of the point of zero charge (pH_{PZC}) is used for that purpose in addition, it can be used to comprehending the electrostatic interactions of the beads with *Cefotaxime* molecules. The point of zero charge of SPVA/IC nanocomposite beads was found around pH 6.5 while for SPVA/IC/$SZrO_2$-1 and SPVA/IC/$SZrO_2$-2.5 nanocomposite beads was found around pHs 6.1 and 5.3 respectively as shown in Fig. S3 in supplementary information. However, below these values of PZC the surface become positively charged on the other hand, above these values the surface acquired negative charge for the removal of positive molecules. The $SZrO_2$ affects the PZC of SPVA/IC polymeric matrix and due to the greater percent of oxygenated groups content in $SZrO_2$ lowers the value of PZC to 6.1 and 5.3 for SPVA/IC/$SZrO_2$-1 and SPVA/IC/$SZrO_2$-2.5 nanocomposite beads respectively. Two processes are involved in the absorption of *Cefotax-*

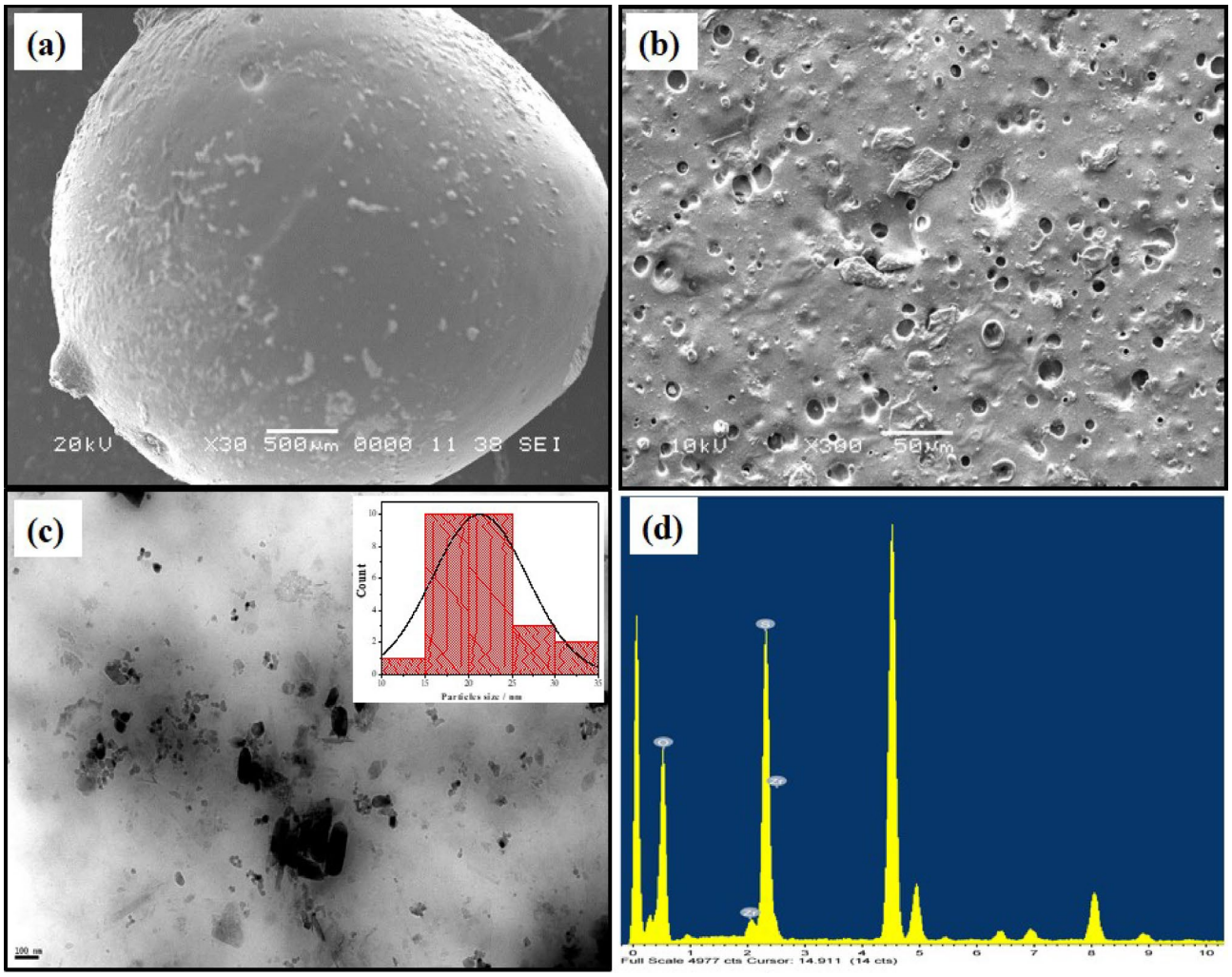

Figure 2. SEM images for (**a**) SPVA/IC/ $SZrO_2$-2.5 beads surface, (**b**) SPVA/IC/ $SZrO_2$-2.5 inside, (**c**) TEM image for $SZrO_2$ nanoparticles with the inset frequency distribution plot of $SZrO_2$ nanoparticles size from TEM image, (**d**) EDX analysis for $SZrO_2$.

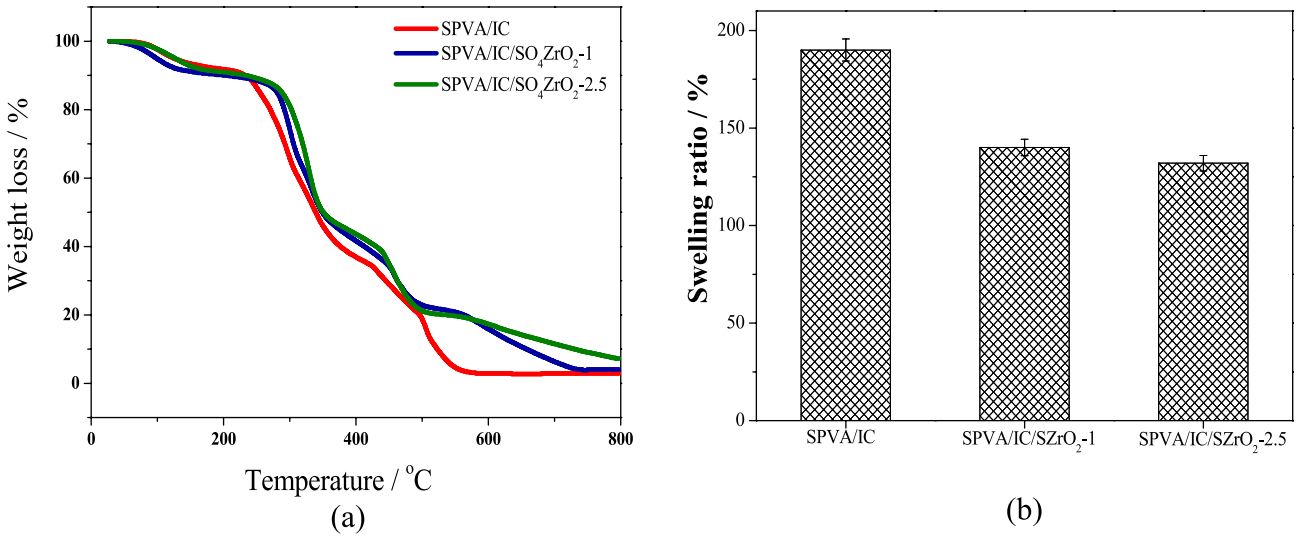

Figure 3. (**a**) TGA curves and (**b**) time dependent swelling response of SPVA/IC and SPVA/IC/$SZrO_2$ nanocomposite beads.

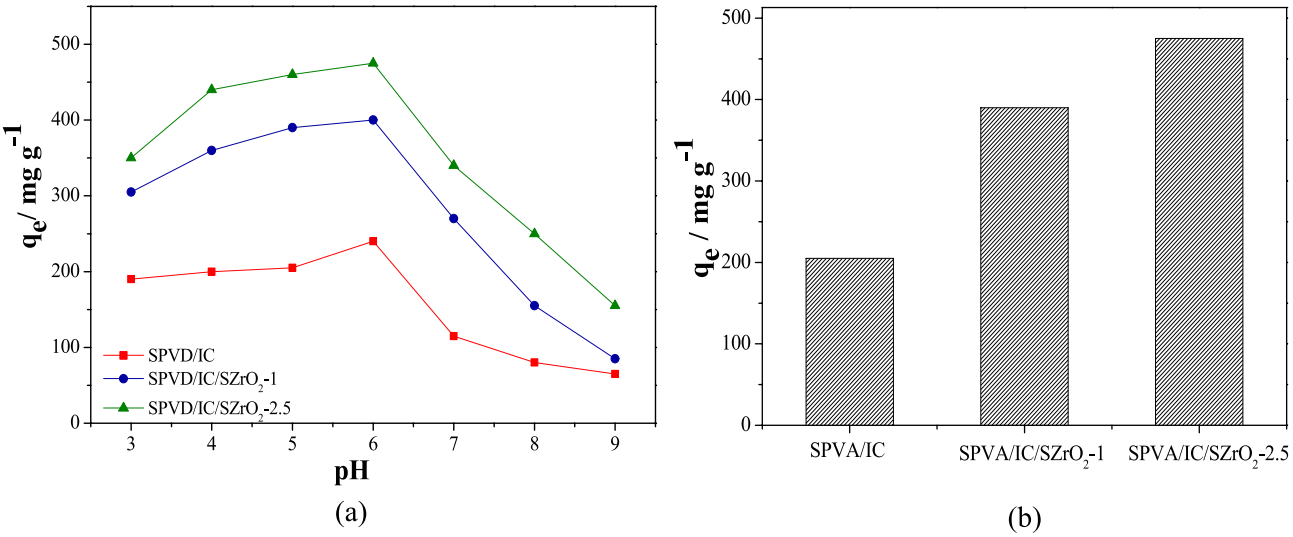

Figure 4. (**a**) Effect of solution's pH (0.01 g adsorbent beads, 50 mL of 100 mg L^{-1} *Cefotaxime* solution at 3 h adsorption time, and 25 °C temperature), (**b**) effect of $SZrO_2$ concentration on *Cefotaxime* adsorption process.

ime from aqueous medium by nanocomposite beads. The first is the diffusion of *Cefotaxime* into nanocomposite beads with water molecule penetration, and the second is associated with electrostatic attractive forces. The pH has a significant and observable impact on the absorption process. The influence of the pH of the solution on *Cefotaxime* adsorption process was studied in the range of 3 to 9 to find the optimal pH value, as shown in Fig. 4a. The results indicate the maximum adsorption has occurred at pH6. The significant decrease of the adsorption capacity at pH ranged between7and 9 may be due to the degradation of *Cefotaxime* followed by hydrolysis of the β-lactam ring and the acetoxy ester. In addition, increasing pH elevate the deprotonation of *Cefotaxime*, accordingly that will increase the repulsion between *Cefotaxime* molecules and negatively charged beads above its PZC values. On the other hand, at very low pH values less than 4, the protonation rate of *Cefotaxime* amine groups will increased, which increases its solubility and decreases its adsorption rate, besides the surfaces of SPVA/IC/$SZrO_2$ would be surrounded by many hydronium ions that compete with *Cefotaxime* for active sites. While, the high adsorption capacity at solution pH ranged between 4 and 6 can be referred to maximum stability of *Cefotaxime* at pH ranged between 4 and 6 (pKa for *Cefotaxime* is 3.1)[28] and that increase the possibility to form hydrogen bond and electrostatic attraction between nanocomposite beads and *Cefotaxime* molecules as shown in Fig. S4 in supplementary information. Thus, pH6 was selected for further adsorption studies of *Cefotaxime*.

A batch adsorption process was used to investigate the effect of adding $SZrO_2$ with different concentrations on *Cefotaxime* adsorption process onto polymeric beads. As shown in Fig. 4b it can be noted that the adsorption capacity of the beads was increased with increasing $SZrO_2$ content and that may be referred to forming hydrogen bond and electrostatic attraction force between oxygenated groups of the composite and amino groups in *Cefotaxime*.

Effect of contact time. As shown in Fig. 5, for all beads samples, the adsorption capacity grew significantly at first, then gradually increased and eventually became constant over time. This could be due to the fact that there are free surface sites available for adsorption during the initial adsorption stage, but due to repulsive forces between *Cefotaxime* molecules adsorbed on beads and those in the solution, the remaining unoccupied surface sites are difficult to utilize as time passes. However, the adsorption process reached equilibrium after approximately 3 h. Furthermore, it can be also noticed the removal efficiency of *Cefotaxime onto* SPVA/IC/$SZrO_2$-2.5 is higher than SPVA/IC and SPVA/IC/$SZrO_2$-1 and that may referred to SPVA/IC/$SZrO_2$-2.5 contain more active side than the other types of beads.

The RSM is a model based on statistics and it is often used to clarify the interaction between reaction parameters for optimization since it is faster, practical and all of the components' effects and potential interactions may be evaluated. The adsorption of *Cefotaxime* onto SPVA/IC/$SZrO_2$-2.5 nanocomposite beads was evaluated according to matrix design illustrated in Table S2 in supplementary information using independent variables including (A) time in hours, (B) *Cefotaxime* concentration in mg L^{-1} and (C) beads dosage in mg on dependent response, which is removal efficiency (%). To explain *Cefotaxime* elimination using SPVA/IC/$SZrO_2$-2.5 beads, the following regression equation for the link between response and variables (A, B and C) was utilized:

$$Removal\ (\%) = 95 + 6.21A - 11.25B + 17.46C + 5AB - 2.08AC + 10BC - 9.04A^2 + 0.5375B^2 - 13.04C^2$$

Moreover, according to the perturbation plot for *Cefotaxime* removal efficiency with SPVA/IC/$SZrO_2$-2.5 nanocomposite beads as shown in Fig. 6, it was observed that as *Cefotaxime* concentrations increases the removal efficiency decreases, while factors time and beads dose have significant effect on removal efficiency whereas they increase, the removal efficiency increased and then decreased.

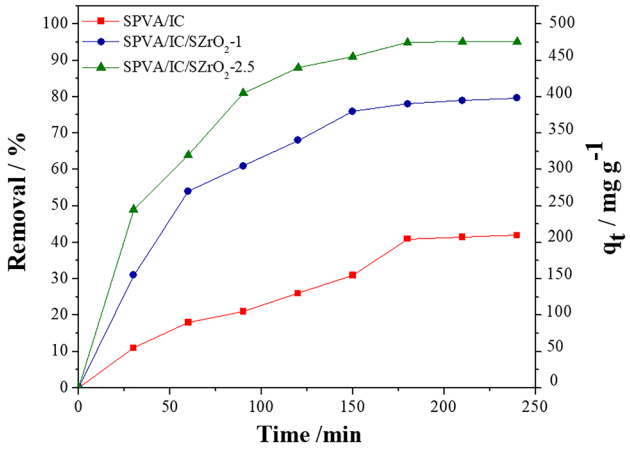

Figure 5. Adsorption kinetics of *Cefotaxime* onto composite beads at C_0; 100 mg L^{-1}, dose of adsorbent beads 0.2 mg mL^{-1}, at 25 °C and pH 6.

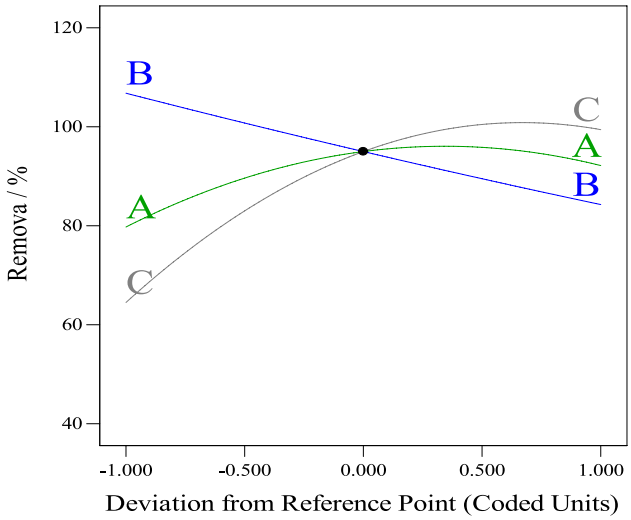

Figure 6. The perturbation plot.

ANOVA analysis of variance is well-known for determining the statistical significance of the quadratic response surface model. As shown in Table S3, the quadratic model is very suitable for high coefficient of determination R^2 (0.9566). The p value of the quadratic model was less than 0.05, therefore, this quadratic model was found to be significant in addition this model is confirmed due to the F-value is found to be 17.16.

According to RSM analysis results as shown in Fig. 7, the following are the optimum conditions: initial *Cefotaxime* concentration is 88.97 mg L^{-1} at time: 3.58 h and adsorbent dosage: 11.68 mg to achieve full removal. The efficiency of *Cefotaxime* elimination was discovered to be impacted by all variable parameters.

Kinetics and isotherms of adsorption process. Three kinetic models were used to study the adsorption of *Cefotaxime* onto SPVA/IC/$SZrO_2$-2.5 nanocomposite beads: pseudo-first-order, pseudo-second-order, and intraparticle diffusion models. For the three kinetic models at varying concentrations, the calculated sorption capacities, reaction rate constants, and R^2 values of the linear correlation coefficients were shown in Table 2. The sorption capacities estimated using the pseudo-first-order equation were found to be significantly different from the experimental results. While, for the pseudo-second-order kinetic model, the resulting R^2 values are generally greater than those obtained from pseudo-first-order kinetics, implying that the sorption process followed pseudo-second-order kinetics and that chemisorption was the rate-controlling phase. This appears to include valence forces as a result of chemical reactions or electron exchange between oxygenated groups on *Cefotaxime* molecules and hydroxyl groups on nanocomposite beads and that were responsible for the hydrogen bonds. Despite the fact that the pseudo-second-order-kinetics model had the best fit order, the findings produced from this model were insufficient to evaluate *Cefotaxime* molecules' diffusion mechanism onto SPVA/IC/$SZrO_2$-2.5 nanocomposite beads. As shown in Fig. S5 in supplementary information, the adsorption process linear fitting findings were consistent with the intraparticle diffusion model, whereas the diffusion mechanism was split into

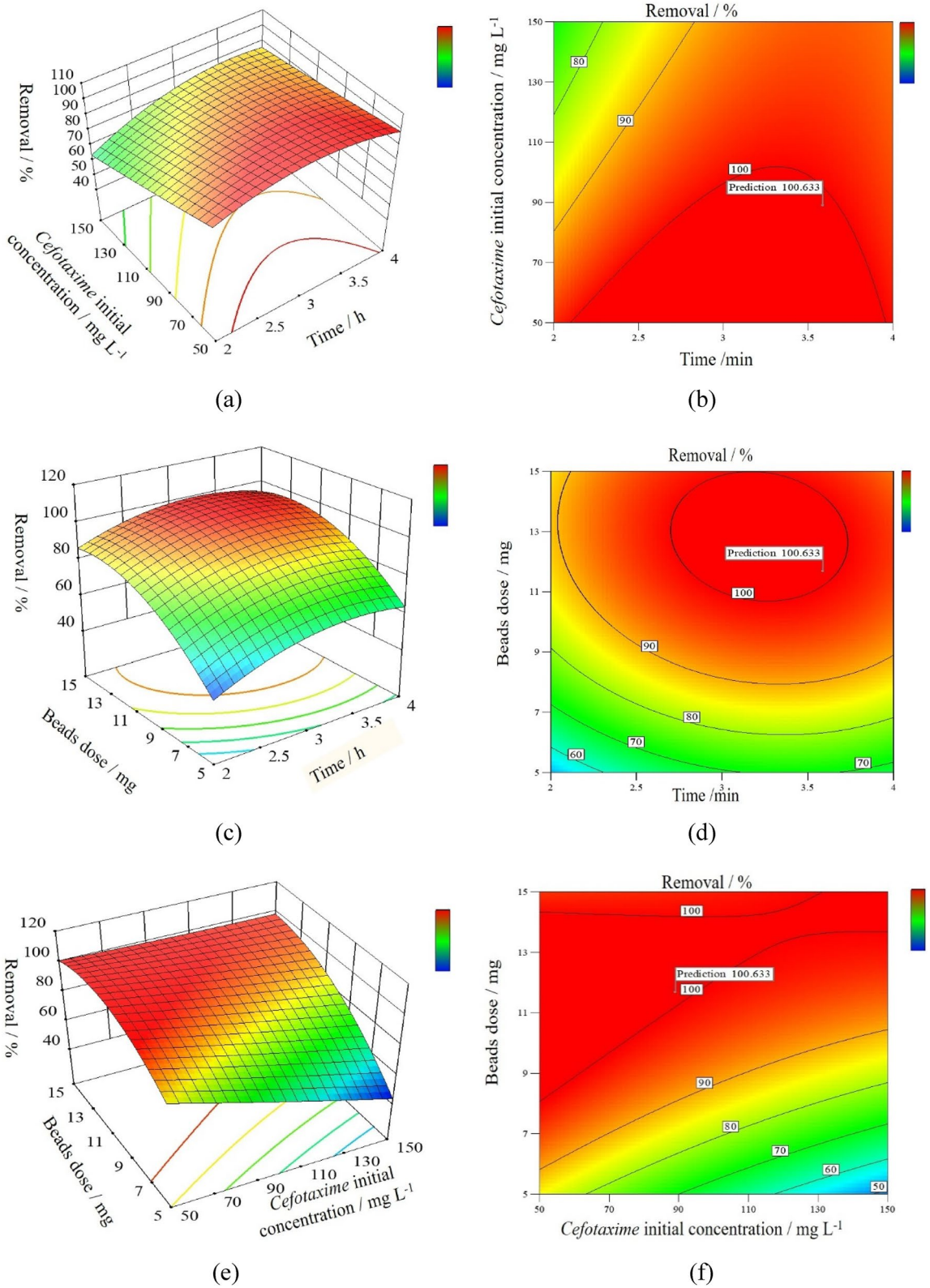

Figure 7. Response surface plots for removal efficiency (%) of *Cefotaxime* onto SPVA/IC/$SZrO_2$-2.5 nanocomposite beads (**a,c,e**) 3D surface plots and (**b,d,f**) 2D surface plots.

three stages that could be explained by the following. At the beginning *Cefotaxime* molecules transport through the solution to the bead surface and form film diffusion at the boundary layer, or charged molecules diffuse

	Cefotaxime initial concentrations (mg L^{-1}) adsorbed onto SPVA/IC/$SZrO_2$-2.5 nanocomposite beads		
	50	**100**	**150**
$q_{e,exp}$ (mg g^{-1})	246	475	659
Pseudo-1st-order			
$q_{e'cal}$ (mg g^{-1})	249.98	476.6	664.1
k_1(min^{-1})	0.031	0.031	0.035
R^2	0.76	0.94	0.85
Pseudo-2nd-order			
$q_{e,cal}$ (mg g^{-1})	245.8	476.1	658.7
k_2(min^{-1})	0.0038	0.0019	0.0013
R^2	0.989	0.981	0.972
Intraparticle diffusion model			
k_i			
$k_{i,1}$	15.16	31.13	64.48
$k_{i,2}$	12.88	18.24	17.25
$k_{i,3}$	1.89	0.48	2.4
C	45.69	56.84	64.48
R^2	0.92	0.87	0.94

Table 2. Kinetic models' parameters and determination coefficients for *Cefotaxime* adsorption onto SPVA/IC/$SZrO_2$-2.5 nanocomposite beads.

	Ciprofloxacin adsorption onto FMFNs		
Temperature °C	**20 °C**	**30 °C**	**40 °C**
Langmuir isotherm			
q_m (mg g^{-1})	735	752	752
k_L(L mg^{-1})	0.49	0.57	0.98
R^2	0.992	0.997	0.999
R_L	0.1	0. 008	0.005
Freundlich isotherm			
K_F (mg g^{-1})	270	299	330
$1/n_F$	0.32	0.34	0.31
R^2	0.99	0.96	0.85

Table 3. Adsorption isotherm parameters for *Cefotaxime* adsorption onto SPVA/IC/$SZrO_2$-2.5 nanocomposite beads at adsorbent dosage 0.2 mg mL^{-1}.

from a bulk solution to the beads' exterior surface after that the *Cefotaxime* charged molecules transferred into the pores and intraparticular active sites of beads. Finally, the *Cefotaxime* molecules were chemically bound via small pores in the beads, followed by the final equilibrium adsorption.

Langmuir and Freundlich models as shown in Fig. S6 were explored at different beginning concentrations and three different temperatures (25, 35 and 45 °C), as illustrated in Table 3. The high adsorption capacity showed a strong electrostatic contact between *Cefotaxime* molecules and the bending sites of the beads, and the R^2 values of the Langmuir model were extremely near to one. Furthermore, at low temperatures, R_L values were higher than at high temperatures, and its values were found to be between zero and one, indicating that the adsorption process is chemical rather than physical[22]. However, the results showed that the adsorption process onto beads was best fitted by Freundlich isotherm model, with values of "n" ranging from 2 to 10, which indicate good adsorption and implying higher efficiency for *Cefotaxime* adsorption by nanocomposite beads as the values get increase.

Desorption–adsorption test. After 10 cycles, the adsorbent's ability to regenerate was tested, and it was observed that the removal efficiency was still high, and that the fluctuations in the removal % after each desorption cycle were quite minor, as shown in Fig. 8, indicating that SPVA/IC/$SZrO_2$-2.5 nanocomposite beads had potential in wastewater application.

The efficiency of prepared SPVA/IC/$SZrO_2$-2.5 nanocompoaite beads for drug removal was compared with other adsorbent materials as illustrated in Table 4.

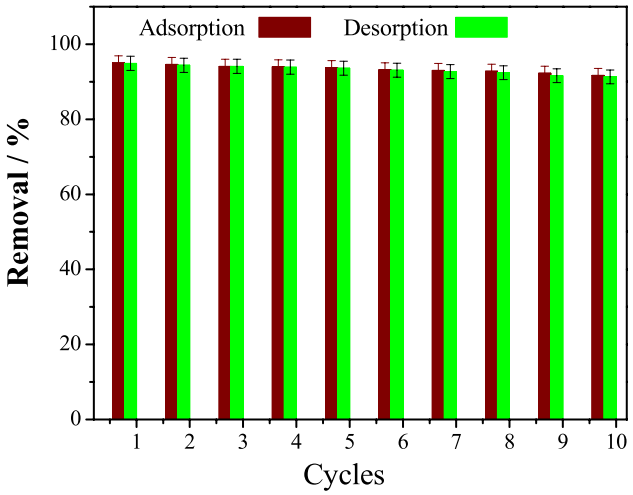

Figure 8. Adsorption–desorption cycles.

Adsorbent nanomaterials	Adsorbate	Optimum adsorption condition	Adsorbate initial concentration (mg L^{-1})	Maximum adsorption capacity (mg g^{-1})	Reusability cycles/ removal% after last cycle	References
Artich-Bch-NaOH	Metformin hydrochloride (MFH)	Acidic medium, 45 min	10	~17	5 cycles, 78.5%	29
NBent-NTiO_2-Chit nanocomposite	Levofloxacin (LEVO) Ceftriaxone (CFT)	pH4, 10 min pH5, 10 min	5	~43 ~36	3 cycles, 95% 3 cycles, 92.8%	30
NFe_3O_4@Zn(GA)/Starch-Hydrogel	Fluvastatin (FLV)	pH2, 30 min	40	~782	5 cycles, 700 mg g^{-1}	31
V_2O_5@Ch/Cu-TMA nanobiosorbent	levofloxacin (LEVO)	pH3, 30 min	10	~9	4 cycles, 84.35%	32
Fe_3O_4–MoO_3-AC	Ciprofloxacin (CPF)	pH7, 30 min	10	~19	5 cycles, 90.5%	33
SPVA/IC/SZrO_2-2.5 nanocompoaite	Cefotaxime	pH6, 3 h	100	~475	10 cycles, 91%	This work

Table 4. A review of the performance of some nanocomposite adsorbent materials used to remove drug from water.

Conclusions

Novel and low expensive nanocomposite beads was produced using a simple blending, eco-environmentally approach and available polymers as PVA and IC. It was appeared that the incorporation of different weight ratio of SO_4ZrO_2 as doping agent into the polymeric PVA/IC blend improves the nanocomposite beads adsorption capacity towards *Cefotaxime* antibiotic. It was discovered that when the ultimate concentration of 100 mg L^{-1} *Cefotaxime* solution was compared at varied contact times and pH 6 conditions, the outcomes were better in the case of SPVA/IC/SZrO_2-2.5 nanocomposite beads. The increasing of SO_4ZrO_2 content in the PVA/IC matrix increases porosity and active functional groups such as oxygen containing groups, so that the adsorption efficiency improves. At various experimental conditions, the time-dependent adsorption capacity was assessed. According to the experimental optimization, it was observed that as *Cefotaxime* concentrations increases the removal efficiency decreases, while factors time and beads dose have significant effect on removal efficiency whereas they increase, the removal efficiency increased and then decreased. The adsorption kinetic of *Cefotaxime* was better fitted to pseudo-second-order model, and the adsorption isotherm was better fitted to the Langmuir and Freundlich models. The ability of SPVA/IC/SZrO_2-2.5 nanocomposite beads to regenerate ten times further demonstrated its suitability for long-term use. The current study reveals that SPVA/IC/SZrO_2-2.5 nanocomposite beads have a lot of potential in water treatment for removing antibiotic pollutants because of their fast separation, ease of operation, high capture capacity, and good cycle performance.

Data availability

All data generated or analyzed during this study are included in this published article and its supplementary information files.

Received: 8 April 2022; Accepted: 11 July 2022
Published online: 26 July 2022

References

1. Nogueira, J. *et al.* Porous Carrageenan-derived carbons for efficient ciprofloxacin removal from water. *Nanomaterials* **8**, 1004 (2018).
2. Sousa, J. C. G., Ribeiro, A. R., Barbosa, M. O., Pereira, M. F. R. & Silva, A. M. T. A review on environmental monitoring of water organic pollutants identified by EU guidelines. *J. Hazard. Mater.* **344**, 146–162 (2018).
3. Teodosiu, A., Gilca, A., Barjoveanu, G. & Fiore, S. Emerging pollutants removal through advanced drinking water treatment: A review on processes and environmental performances assessment. *J. Clean. Prod.* **197**, 1210–1221 (2018).
4. Gavrilescu, M., Demnerová, K., Aamand, J., Agathos, S. & Fava, F. Emerging pollutants in the environment: Present and future challenges in biomonitoring, ecological risks and bioremediation. *Nat. Biotechnol.* **32**, 147–156 (2015).
5. Windsor, F. M., Ormerod, S. J. & Tyler, C. R. Endocrine disruption in aquatic systems: Up-scaling research to address ecological consequences. *Biol. Rev.* **93**, 626–641 (2018).
6. Deblonde, T., Cossu-Leguille, C. & Hartemann, P. Emerging pollutants in wastewater: A review of the literature. *Int. J. Hyg. Environ. Health* **214**, 442–448 (2011).
7. Paíga, P. *et al.* Assessment of 83 pharmaceuticals in WWTP influent and effluent samples by UHPLC-MS/MS: Hourly variation. *Sci. Total Environ.* **648**, 582–600 (2019).
8. Li, Z. *et al.* Removal and adsorption mechanism of tetracycline and cefotaxime contaminants in water by NiFe2O4-COF-chitosan-terephthalaldehyde nanocomposites film. *Chem. Eng. J.* **382**, 123008 (2020).
9. Miyata, M., Ihara, I., Yoshid, G., Toyod, K. & Umetsu, K. Electrochemical oxidation of tetracycline antibiotics using a Ti/IrO_2 anode for wastewater treatment of animal husbandry. *Water Sci. Technol.* **63**, 456–461 (2011).
10. Ahmad, R., Ansari, K. & Ejaz, M. O. Enhanced sequestration of heavy metals from aqueous solution on polyacrylamide grafted with cell@Fe_3O_4 nanocomposite. *Emergent Mater.* https://doi.org/10.1007/s42247-021-00338-8 (2022).
11. Osman, M. *et al.* Metal sorption, solid phase extraction and preconcentration properties of two silica gel phases chemically modified with 2-hydroxy-1-naphthaldehyde. *Microchim. Acta* **143**, 25–31 (2003).
12. MohyEldin, M. S., Gouda, M. H., Abu-Saied, M. A., El Shazly, Y. M. S. & Farag, H. A. Development of grafted cotton fabrics ions exchanger for dye removal applications: Methylene blue model. *Desal. Wat. Treat.* **57**, 22049–22060 (2016).
13. Elessawy, N. A. *et al.* Sustainable microbial and heavy metal reduction in water purification systems based on PVA/IC nanofiber membrane doped with PANI/GO. *Polymers* **14**, 1558 (2022).
14. Mahmoud, M. E. *et al.* Novel immobilized fibrous natural cotton on *Corchorus olitorius* stalks biochar@diethylenetriamine@feroxyhyte@diethylenetriamine composite for coagulative removal of silver quantum dots (Ag-QDs) from water. *Cellulose* **28**, 11397–11416 (2021).
15. Mahmoud, M. E., Abouelanwar, M. E., Mahmoud, S. M. E. & Salam, M. A. Doping starch-gelatin mixed hydrogels with magnetic spinel ferrite@biochar@ molybdenum oxide as a highly efficient nanocomposite for removal of lead (II) ions. *J. Environ. Chem. Eng.* **9**, 106682 (2021).
16. Gouda, M. H. *et al.* Novel nanocomposite membranes based on cross-linked eco-friendly polymers doped with sulfated titania nanotubes for direct methanol fuel cell application. *Nanomater. Nanotechnol.* **10**, 1–9 (2020).
17. Nanaki, S. G. *et al.* Synthesis and characterization of modified carrageenan microparticles for the removal of pharmaceuticals from aqueous solutions. *Colloids Surf. B Biointerfaces* **127**, 256–265 (2015).
18. Zhuang, Y., Yu, F., Ma, J. & Chen, J. Enhanced adsorption removal of antibiotics from aqueous solutions by modified alginate/graphene double network porous hydrogel. *J. Colloid Interface Sci.* **507**, 250–259 (2017).
19. Jhaveri, J. H. & Murthy, Z. V. P. A comprehensive review on anti-fouling nanocomposite membranes for pressure driven membrane separation processes. *Desalination* **379**, 137–154 (2016).
20. Pang, R. *et al.* Preparation and characterization of ZrO_2/PES hybrid ultrafiltration membrane with uniform ZrO_2 nanoparticles. *Desalination* **332**, 60–66 (2014).
21. Monsef, K., Homayoonfal, M. & Davar, F. Coating carboxylic and sulfate functional groups on ZrO_2 nanoparticles: Antifouling enhancement of nanocomposite membranes during water treatment. *React. Funct. Polym.* **131**, 299–314 (2018).
22. Gouda, M. H., Elessawy, N. A. & Santos, D. M. F. Synthesis and characterization of novel green hybrid nanocomposites for application as proton exchange membranes in direct borohydride fuel cells. *Energies* **13**, 1180 (2020).
23. Mahmoud, M. E. *et al.* Performance of MnO_2 nanoparticles-coated cationic CTAB for detoxification and decolorization of sulfonated remazol red and reactive black 5 dyes from water. *Int. J. Environ. Sci. Technol.* **19**, 141–158 (2022).
24. Box, G. & Behnken, D. W. Some new three level designs for the study of quantitative variables. *Technometrics* **2**, 455–475 (1960).
25. Ye, Y. S. *et al.* Alkali doped polyvinyl alcohol/graphene electrolyte for direct methanol alkaline fuel cells. *J. Power Sources* **239**, 424–432 (2013).
26. Papageorgiou, M. *et al.* Novel isocyanate-modified carrageenan polymer materials: Preparation, characterization and application adsorbent materials of pharmaceuticals. *Polymers* **9**, 595 (2017).
27. Sonal, S., Singh, A. & Mishra, B. K. Decolorization of reactive dye Remazol Brilliant Blue R by zirconium oxychloride as a novel coagulant: Optimization through response surface methodology. *Water Sci. Technol.* **78**, 379–389 (2018).
28. Nodeh, H. R. & Sereshti, H. Synthesis of magnetic graphene oxide doped with strontium titanium trioxide nanoparticles as a nanocomposite for the removal of antibiotics from aqueous media. *RSC Adv.* **6**, 89953 (2016).
29. Mahmoud, M. E., El-Ghanam, A., Saad, S. R. & Mohamed, R. H. A. Promoted removal of metformin hydrochloride anti-diabetic drug from water by fabricated and modified nanobiochar from artichoke leaves. *Sustain. Chem. Pharmacy.* **18**, 100336 (2020).
30. Mahmoud, M. E., El-Ghanam, A., Mohamed, R. H. A. & Saad, S. R. Enhanced adsorption of Levofloxacin and Ceftriaxone antibiotics from water by assembled composite of nanotitanium oxide/chitosan/nano-bentonite. *Mater. Sci. Eng. C* **108**, 110199 (2020).
31. Mohamed, A. K. & Mahmoud, M. E. Encapsulation of starch hydrogel and doping nanomagnetite onto metal-organic frameworks for efficient removal of fluvastatin antibiotic from water. *Carbohyd. Polym.* **245**, 116438 (2020).
32. Mahmoud, M. E., Amira, M. F., Azab, M. M. H. M. & Abdelfattah, A. M. Effective removal of levofloxacin drug and Cr(VI) from water by a composed nanobiosorbent of vanadium pentoxide@chitosan@MOFs. *Int. J. Biol. Macromol.* **188**, 879–891 (2021).
33. Mahmoud, M. E., Saad, S. R., El-Ghanam, A. & Mohamed, R. H. A. Developed magnetic Fe3O4–MoO3-AC nanocomposite for effective removal of ciprofloxacin from water. *Mater. Chem. Phys.* **257**, 123454 (2021).

Author contributions

The manuscript was written through the contributions of all authors. All authors have approved the final version of the manuscript.

Funding

Open access funding provided by The Science, Technology & Innovation Funding Authority (STDF) in cooperation with The Egyptian Knowledge Bank (EKB).

Competing interests
The authors declare no competing interests.

Additional information
Supplementary Information The online version contains supplementary material available at https://doi.org/10.1038/s41598-022-16473-z.

Correspondence and requests for materials should be addressed to N.A.E.

Reprints and permissions information is available at www.nature.com/reprints.

Publisher's note Springer Nature remains neutral with regard to jurisdictional claims in published maps and institutional affiliations.